Wormlike micelles under shear flow: A microscopic model studied by nonequilibrium-molecular-dynamics computer simulations

M. Kröger*
Institut für Theoretische Physik, Technische Universität Berlin, PN 7-1, Hardenbergstrasse 36, D-10623 Berlin, Germany

R. Makhloufi
Laboratoire de Physique des Liquides et Interfaces, Groupe Physique des Colloides et Polymères, Université de Metz, 1 Boulevard Arago, 57078 Metz Cedex 03, France

(Received 24 July 1995)

We propose a microscopic model for solutions of wormlike micelles and report results from nonequilibrium-molecular-dynamics computer simulations under shear flow. Our model ("FENE-C") introduces the concept of scission-recombination and is an extension of a recent model employed by one of us [M. Kröger, Rheologie und Struktur von Polymerschmelzen (Wissenschaft and Technik, Berlin, 1995); Rheology **5**, 66 (1995)] for polymer melts. In this study our interest is focused on the relevance of the microscopic model by comparing the results of the simulations with the predictions of mesoscopic theories. The simulated behavior shows an exponential distribution for the micellar length and an exponential dependence of the average length on the scission energy at equilibrium. These results correspond to those calculated from Cates mesoscopic theory. Results of simulations concerning the effect of shear flow on the size distribution and on the average length of the micelles are also reported and discussed.

PACS number(s): 61.25.Hq, 83.50.Ax, 61.20.Gy, 61.20.Ja

I. INTRODUCTION

Aqueous surfactant solutions are known to form elongated micelles under certain thermodynamic conditions characterized by surfactant concentration, salinity, or temperature [1,2]. In the semidilute regime these linear and flexible particles, with persistence lengths varying from 15 to 150 nm [3], form an elongated viscoelastic network. In equilibrium their behavior is analogous to that of polymer solutions and their properties obey the scaling laws predicted for the semidilute range [4]. This analogy is now well understood. In contradistinction to ordinary polymers, these wormlike micelles can break and recombine within a characteristic time (breaking time) and their micellar length obeys an exponential distribution [5].

As a consequence of this scission-recombination process and polydispersity, the flow properties of these living polymers show characteristic behaviors, often different from those of classical polymers. Recently observed phenomena such as shear banding structure, shear inducing structure, phase transitions, and thixotropy [6–9] are not completely understood; for example, the data are interpreted without taking into account the possible effect of flow on the size of the micelles or on their polydispersity (distribution of lengths [10,11]).

This effect has been considered theoretically by Wang, Gebart, and Ben-Shaul [12] for dilute solutions of rodlike micelles. Their model predicts a reduction of the micellar size under extensional flow. In a later work on rodlike micelles Wang [13] found that under shear flow, above a certain critical shear rate, a gel-like molecular structure appears. Recently, the same author, using a nonequilibrium-statistical-mechanic approach, has reported that rodlike micelles grow at high shear rates [14]. This result is, however, different from that reported experimentally by Rehage, Wunderlich, and Hoffmann [15].

Until now there exists no general theory of these flow effects and the understanding of these phenomena is still incomplete [16–19]. The aim of this work is to introduce an approach to study the flow properties of micellar systems. We propose a microscopic model for wormlike micelles, which we study by nonequilibrium-molecular-dynamics (NEMD) computer simulations. The aim of using such a powerful tool is to help to understand the microscopic origin of flow phenomena in micellar systems.

Our model ("FENE-C") introduces the concept of scission recombination of the micelles and it is an extension of a model established recently for polymers in equilibrium [20] and under flow [21,22]. Preliminary simulations results on polymer melts under shear flow were published by Hess [23].

In this study on systems of flexible micelles our interest is focused on the relevance of the microscopic model by comparing the equilibrium properties of the simulations (distribution of length and mean length) with those calculated from mesoscopic theories. Moreover, the effect of shear flow on these quantities is analyzed.

This article proceeds as follows. In Sec. II the main predictions on the equilibrium properties as predicted by the mesoscopic theory are briefly recalled. In Sec. III the microscopic FENE-C model is presented. In Secs. IV

*Author to whom correspondence should be addressed. FAX: +49 +30 314 21130. Electronic address: mk@polly.physik.tu-berlin.de.

 ©1996 The American Physical Society

and V the results of the simulations will be reported and discussed.

II. EQUILIBRIUM PROPERTIES FROM THE MESOSCOPIC THEORY

From a mean-field (Flory-Huggins) approach Cates [5] has calculated the equilibrium properties of reversibly breaking aggregates such as micelles. He found that the normalized number density $C(L)$ of micelles of length L (L is equal to the number of monomers units in a chain) is given by an exponential function

$$C(L) \propto \exp\left[-\frac{L}{\bar{L}}\right], \tag{1}$$

with a mean length $\bar{L}$ given by

$$\bar{L} \propto \phi^{1/2} \exp\left[\frac{E_{sc}}{2k_B T}\right], \tag{2}$$

where ϕ represents the total volume fraction, and E_{sc} the scission energy, which is the energy required to create two chain ends (or to break a chain into two parts), and T denotes the absolute temperature.

In this model, it is assumed that a chain can break (and recombine) with a fixed probability per unit time per unit length anywhere along its length. Successive breakage and recombination events are not correlated. This reversible unimolecular process is characterized by a rate constant k_1 and by a micellar breaking time τ_b (time separating two successive scissions) related to the mean length $\bar{L}$ by

$$\tau_b = \frac{1}{k_1 \bar{L}} . \tag{3}$$

III. THE MICROSCOPIC FENE-C MODEL

A. Nonequilibrium molecular dynamics

Newton's equations of a (classical) many-particle problem under external forces can be solved iteratively by NEMD computer simulations. For the case studied here, the external forces build up a macroscopic velocity gradient (with shear rate as parameter) in the fluid. During the simulation the extraction of physical quantities is performed by following the concepts of statistical physics. The quantities of both macroscopic and microscopic interest are expressed in terms of the configurational quantities such as the space coordinates or velocities of all (interacting) particles. Therefore the NEMD method serves as an instrument to investigate the molecular sources of macroscopically measurable transport phenomena [26]. To perform simulations of physical relevance they have to be based on simple models. It is a permanent element of progress to check the relevance by comparison with experimental results [12,27,28].

B. Microscopic model for wormlike micellar solutions

The micellar solution of concentration ϕ is modeled by N_b monomers (particles), which interact via two-body potentials (Fig. 1). Let ϕN_b be the number of particles that are able to form wormlike chains of monomers ("M particles") and $(1-\phi)N_b$ the number of solvent particles ("S particles"). All particles of the system (M and S) have the same mass and interact via the purely repulsive part of the Lennard-Jones (LJ) potential [29]

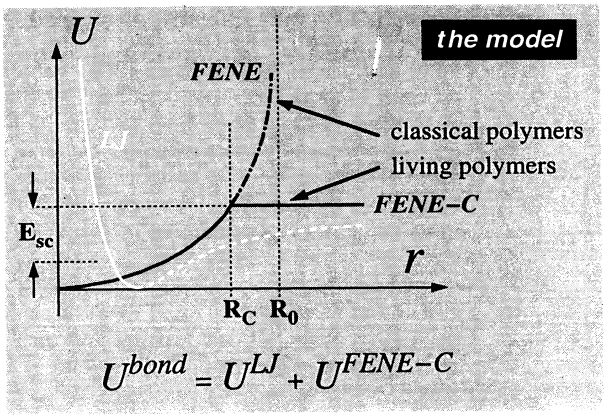

FIG. 1. Model potentials specifying the microscopic model of wormlike micelles. All particles interact via the truncated (repulsive) Lennard-Jones potential. The FENE-C potential produces the bonding interactions.

$$U_{ij}^{LJ} = \begin{cases} 4\epsilon[(r_{ij}^*)^{-12} - (r_{ij}^*)^{-6} + \frac{1}{4}] & \text{for } r_{ij}^* \le r_{cut} = 2^{1/6} \\ 0 \quad \text{for } r_{ij}^* > r_{cut}, \end{cases} \tag{4}$$

with $r_{ij}^* = r_{ij}/\sigma$ being the dimensionless distance between particles i and j. In the following all quantities resulting from the simulations are reduced to LJ units, which provides the energy (by ϵ) and length scale (by σ) of the system; the monomeric mass gives the third unit. A quantity will be indexed by an asterisk, if otherwise ambiguities can occur. For example, the reference quantities for density, temperature, time, and viscosity are

$$\begin{aligned} &n_{ref} = \sigma^{-3}, \quad T_{ref} = \epsilon/k_B , \\ &t_{ref} = \sigma\sqrt{m\epsilon}, \quad \eta_{ref} = \sigma^{-2}\sqrt{m\epsilon} . \end{aligned} \tag{5}$$

All M particles are able to form transient bonds with all other M particles except with those of the same chain, but every M particle can have at maximum two bonds at the same time. Within these conditions, which ensure that only end-to-end recombinations and therefore no branched structures can occur, all M particles interact via the following, now called "FENE-C," potential:

$$U_{ij}^{FENE\text{-}C} \equiv \begin{cases} -0.5k^* R_0^2 \ln[1-(r_{ij}^*/R_0)^2] \\ \qquad \text{for } r_{ij}^* \le \min(R_C, R_0) \\ -0.5k^* R_0^2 \ln[1-(R_C/R_0)^2] \\ \qquad \text{for } r_{ij}^* \ge R_C , \end{cases} \tag{6}$$

with parameters R_0 (maximum bond length), R_C (cutoff radius), and k^* (strength of spring). The corresponding scission energy E_{sc} is connected with the cutoff radius R_C

via the difference between $U^{\text{bond}}(r^* \to \infty)$ and the energy at the minimum of the bonding potential (see Fig. 1). The original FENE potential for a "finitely extendable nonlinear elastic" spring is obtained from the FENE-C potential by setting $R_C = R_0$. The FENE potential was proposed by Warner [30] and used by Ceperly, Kalos, and Lebowitz [31] and Kremer and Grest [20] to study polymer systems in equilibrium. See Fig. 2 for a schematic representation of micellar configurations during possible end-to-end recombination (or after a break). Resulting from the model potentials, a break is favored for a bond that is stretched because of thermal fluctuations, forces due to the velocity gradient or local topological constraints (entanglements). In contrast, the possibility of a subsequent recombination of two ends depends only on the degree of fluctuation of ends, the temporary number density of (open) ends and structural peculiarities, which may favor an instantaneous recombination of broken parts of a micelle. To be able to compare directly with previous results on polymer melts, i.e., "classical polymers" ($R_C = R_0$) with maximal concentration $\phi = 100\%$ as in [8,12], we have chosen $R_0 = 1.5$ and $k^* = 30$ at constant temperature $T^* = 1$ and particle density $n^* = 0.84$. The strength of the spring is small enough to permit a "large" integration time step of $\Delta t^* = 0.005$. The nonlinearity of the FENE potential determines the quality (ergodicity) of the simulation: the phase space is filled better than for the case of an underlying Hookean force law to connect particles within micelles. The results in both cases will show different phenomenology too. Starting from the (classical) Liouville equation, the time evolution of the trajectories of all monomers can be discretized. By expanding the formal solution of that equation to first order in Δt (the time step) one gets the "leapfrog algorithm" [32], from which the presently used "velocity Verlet algorithm" [33] is deduced. All (real) monomers of the simulated system from which physical observables

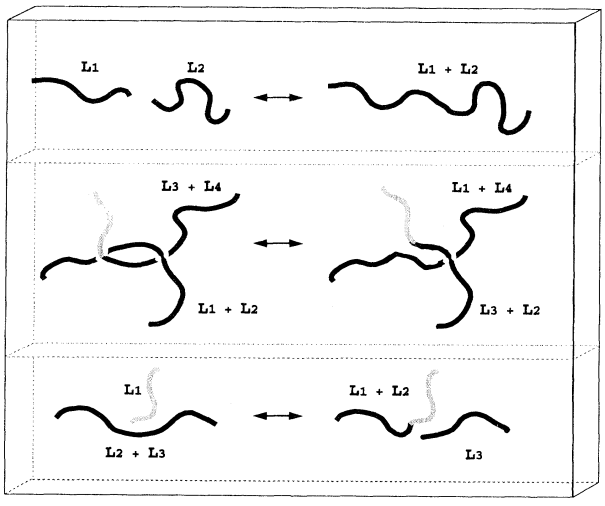

FIG. 2. Schematic representation of micellar configurations during end-to-end recombination (or after a break). Resulting from the model, a break is favored for a bond that is stretched because of thermal fluctuations, forces due to the velocity gradient, or local topological constraints (entanglements).

are obtained are confined within a "central" cubic cell of constant volume. That volume is, together with its particles, periodically reproduced in every direction of space. Particles are allowed to cross the surface and to interact through the surface of the central cell via the "nearest image convention" [33], which is always used when studying bulk properties from molecular-dynamics simulations. Hence a monomer cannot directly interact with its own "image particle" because the cutoff radii of the chosen potentials are smaller than the simulated box length. For the present simulations the volume of the central cell $V^{1/3} \approx 26 \gg \max(R_C, 2^{1/6})$, where $2^{1/6}$ is the minimum of the LJ potential. The shear flow is imposed by the homogeneous shear flow algorithm of Evans [34]. During the simulation the temperature is kept constant by rescaling the peculiar velocities as described in [23].

The ideal FENE-C potential leads to a discontinuity in acceleration of particles at the moment of recombining and breaking. In view of our investigations with a set of smoothing functions, defined on the interval $[R_C - \Delta R, R_C + \Delta R]$ with $\Delta R \leq 0.01$, there is no need to specify further the model potential by introducing more parameters describing a smoothing of the potential in the vicinity of the radius R_C. We checked that all measured macroscopic quantities are insensitive to the exact trajectories within the corresponding time interval of one scission or one recombination process, respectively, resulting from its small value compared with the breaking and relaxation times of chains. These results are not reported here.

All simulated systems presented here consist of $N_b = 8400$ monomers. Neighbor lists and layered link cells [35] are used to optimize the computer routines. In contrast to the equilibrium simulations the list of pair dependences is updated based on an upper limit for the increase of the relative separation of these pairs, not on the absolute motion of individual particles. Starting from equilibrated samples the typical times t^* required to reach a steady state varied from $t^* = 10^3$ for $\phi = 4\%$ at the highest shear rate $\gamma = 2$ to $t^* = 2 \times 10^4$ for $\phi = 100\%$ at the lowest shear rate $\gamma = 10^{-4}$. As checked by the inverse experiment, the stress relaxation times after sudden cessation of steady-state shear flow are smaller than the chosen time intervals: e.g., the relaxation times t^*_{relax} of samples with $\phi = 4\%$ and 100% after cessation of shear with $\gamma = 0.01$ are $t^*_{\text{relax}} = 250 \pm 50$ and 2800 ± 700, respectively. The CPU time used per time step was 0.041 s on a CRAY Y-MP supercomputer for a system with 8400 beads.

IV. COMPUTER SIMULATIONS RESULTS

By varying the cutoff radius R_C of the intramolecular FENE-C potential the results for simple fluids [24] and polymer melts [21,25] can be reproduced in the limiting cases of $R_C = 0$ and $R_C = R_0$, respectively. In order to analyze living polymer systems consisting of "long" chains, i.e., with $\bar{L} > 10$ and $\bar{L} < 120$ (which is a large value in view of the chosen size of the central cell), we chose $R_c = 1.13$ (compare with Fig. 3 and Table I) to produce most of the presented data.

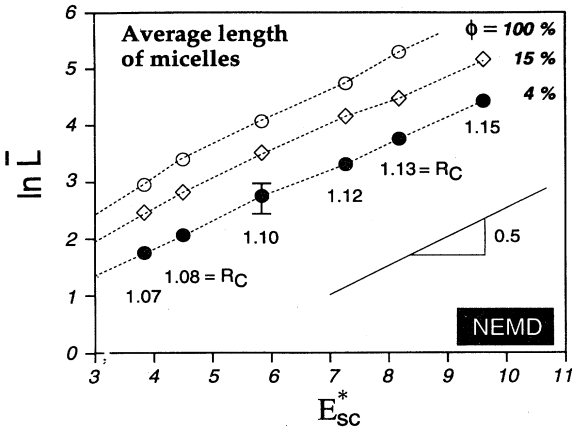

FIG. 3. Average micellar length $\bar{L}$ vs the scission energy for micellar solutions (from 4% to 100%) in equilibrium.

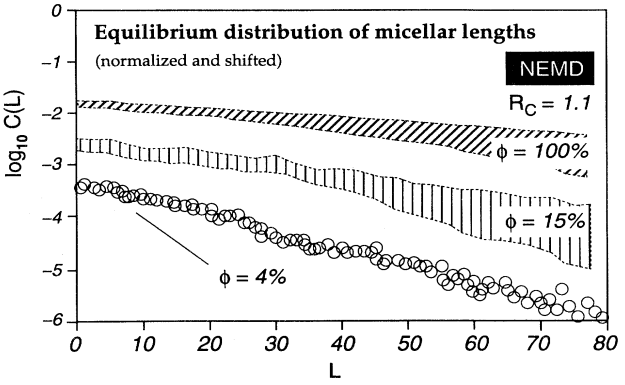

FIG. 4. Normalized equilibrium distribution of micellar length $C(L)$ for samples $S1$, $S3$, and $S5$. All samples are characterized further in Table I.

A. Equilibrium properties

The simulation results on equilibrated sample ($\Delta t^*_{eq} = 2\times 10^5$) properties are characterized by the distribution of length $C(L)$ and the average micellar length $\bar{L}$ against the scission energy E_{sc}. These curves are plotted in Figs. 3 and 4. The exponential form of these two quantities, which represents a large polydispersity of the living

TABLE I. Relevant equilibrium properties for five samples, $S1$–$S4$ (solutions) and $S5$ (polydisperse melt). For given concentration ϕ, cutoff parameter R_C of the FENE-C potential and the corresponding scission energy E_{sc}, the breaking time for micelles τ_b (equal to the recombination time τ_r in equilibrium), and the average length of micelles $\bar{L}$ as well as the quantity k_1 as defined by $k_1^{-1} = \bar{L}\tau_b$, all shown at different shear rates $\dot{\gamma}$.

Parameters / Samples	$S1$	$S2$	$S3$	$S4$	$S5$
ϕ	4%	4%	15%	50%	100%
R_C	1.10	1.13	1.13	1.13	1.13
E_{sc}	5.86	8.09	8.09	8.09	8.09
		$\dot{\gamma}=0$			
$\bar{L}$	13	38	52	134	210
τ_b	10.4	27.0	18.7	5.8	3.4
$10^3 k_1$	9.8	1.07	1.16	1.21	1.39
		$\dot{\gamma}=0.01$			
$\bar{L}$	12.4	31	45	110	182
τ_b	8.5	35	23	6.1	3.6
$10^3 k_1$	9.6	1.08	1.15	1.22	1.45
		$\dot{\gamma}=0.1$			
$\bar{L}$	10.3	24	35	81	111
τ_b	10.4	43	29	9.5	5.0
$10^3 k_1$	9.6	1.16	1.23	1.33	1.59
		$\dot{\gamma}=1.0$			
$\bar{L}$	8.4	12	19	42	85
τ_b	25.6	59	36	11.2	5.5
$10^3 k_1$	8.7	1.43	1.52	1.60	1.71

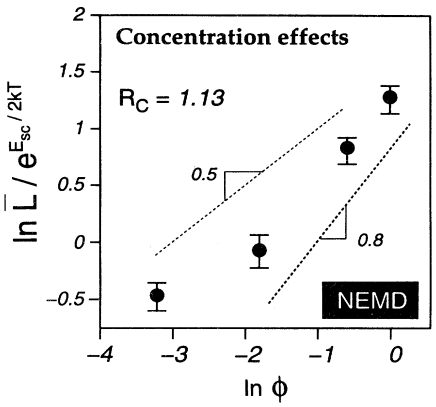

FIG. 5. Average micellar length $\bar{L}$ (reduced) vs the volume fraction ϕ, to be compared with the mesoscopic result [Eq. (2)].

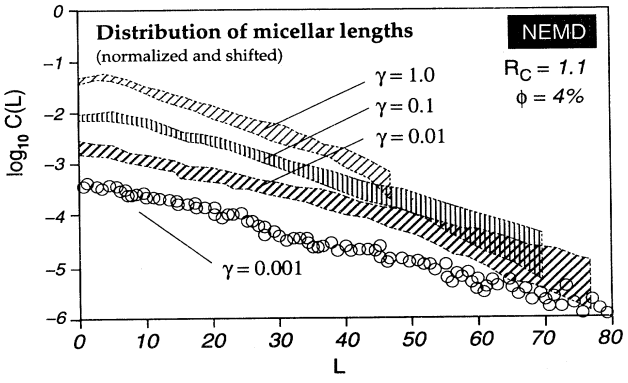

FIG. 6. Normalized distribution of micellar length $C(L)$ at four different shear rates for sample $S1$.

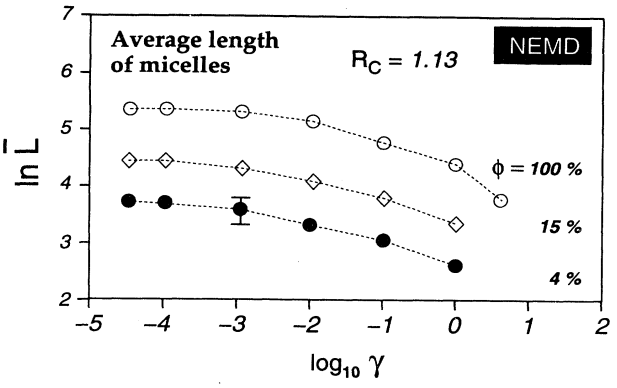

FIG. 7. Average micellar length $\bar{L}$ vs the shear rate for the samples $S2$, $S3$, and $S5$ (see Table I).

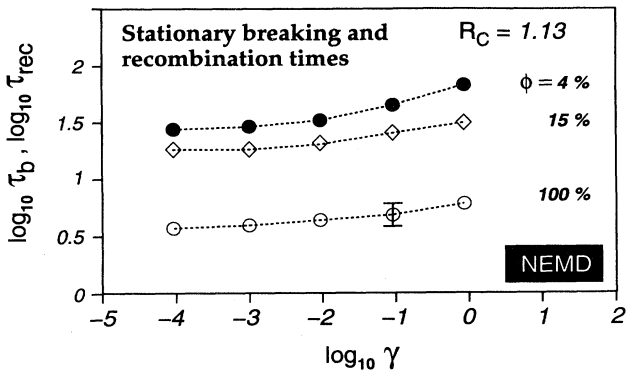

FIG. 8. Average breaking time (equal to the recombination time in the stationary regime) vs shear rate for the same samples as in Fig. 7.

polymer samples and an important dependence of $\bar{L}$ on the scission energy, is quite comparable with predictions of Cates [see Eqs. (1) and (2)]. In particular, these results support the relevance of the microscopic FENE-C model. The concentration dependence of $\bar{L}$, reported in Fig. 5 from three samples (compare with Table I), is found to scale with the volume fraction ϕ with an exponent around 0.5–0.8, as predicted by diverse mean field models [1,36–38]. Notice that there is an indication of a concentration-induced size growth, which is not described by a single power law. At high concentrations the few data points in Fig. 4 seem to be described better by a power law value of 0.7–0.8. Recently, experimental results of Schurtenberger *et al.* [39] indicated an even stronger concentration dependence (≈ 1) for aqueous solutions of the nonionic surfactant hexa-ethylene glycol mono-*n*-hexadecyl ether ($C_{16}E_6$), which forms giant polymerlike micelles in water. Macroscopic quantities, such as the viscosities, the birefringence, or all types of structure factors, can be extracted from the microscopic model without introducing further assumptions, as is necessary in order to simplify the calculation within the mesoscopic approach.

B. Flow effects

The length distributions $C(L)$ for a sample under shear are reported in Fig. 6. The plots of $C(L)$ at different shear creates appear to be qualitatively of the same form as in equilibrium and seem to be unaffected by the flow, except for small lengths. At high shear rates the shortest chains are not as favored as under equilibrium conditions. The small micellar chains, expected to be dynamically aligned to a certain degree under flow, apparently are more stable than single M monomers. Such an effect could be related to the decrease of diffusivity of M monomers, bonded in micellar chains, compared to its free counterparts.

The simulations show a decrease of the mean length of the particles $\bar{L}$ with increasing shear rates (Fig. 7) evolving in the onset of flow, when the number of breaks exceeds the number of recombinations. Because it is difficult to measure directly the micellar mean length experimentally, that effect has not yet been verified. An opposite behavior, the so-called shear induced structure, has been reported by Hoffmann, Rauscher, and Hoffmann [18], where rodlike micelles are found to increase in size under low shears. In our simulations we study long chains and the decrease of $\bar{L}$ occurs at relatively high shear rates. Within the microscopic model this effect should be understood as a consequence of shear-induced stretching of bonds, which in stationary flow is accompanied by an equivalent increase of recombination processes.

As a consequence of the decrease in size, the breaking time shows a tendency to increase slightly at high shear rates. This can be seen from Fig. 8, where this quantity is plotted as a function of the shear rate for different samples. We have summarized finally in Table I the relevant stationary properties for all the samples studied at different shear rates.

V. CONCLUSION

It has been shown that the results of the simulations on the equilibrium properties $C(L)$ and $\bar{L}$ support the relevance of the microscopic FENE-C model in predicting behavior similar to real micellar systems. Its equilibrium properties are comparable with those predicted by the mean field model. The microscopic model presented is adopted to study in detail the underlying molecular mechanisms in equilibrium and the origins of viscoelastic behavior under nonequilibrium conditions without introducing further assumptions into the model. The FENE-C model shows a decrease of the mean length at high shear rates while the distribution of length is quite unaffected by the flow.

In a subsequent study, rheological and structural quantities such as shear viscosities, normal stress differences, static structure factors, and the flow birefringence will be extracted for the case of planar Couette flow, as outlined in [21,22]. A study of the microscopic model under various isochoric time-dependent flows is in progress.

ACKNOWLEDGMENTS

M.K. thanks the Sonderforschungsbereich 335 "Anisotropic Fluids" and the graduate college "Polymerwerkstoffe" (Berlin) of the Deutsche Forschungsgemeinschaft for financial support, as well as the Konrad-Zuse-Zentrum für Informationstechnik (Berlin) and the German supercomputing center (HLRZ) of the KFA Jülich GmbH for their generous donation of CPU time of CRAY Y-MP 4D/464 and on CRAY J916/16-4096 vector machines.

[1] M. E. Cates and S. J. Candau, Condens. Matter **2**, 6869 (1990), and references therein.

[2] H. Rehage and H. Hoffmann, Mol. Phys. **74**, 933 (1991), and references therein.

[3] J. Appel and G. Porte, Europhys. Lett. **12**, 185 (1990); I. Imae, J. Colloid Polym. Sci. **267**, 707 (1989); I. Imae and T. Kohsaka, J. Phys. Chem. **96**, 10 030 (1992).

[4] P. G. de Gennes, *Scaling Concepts in Polymer Physics* (Cornell University Press, Ithaca, 1979).

[5] M. E. Cates, Macromolecules **20**, 2289 (1987); J. Phys. (Paris) **49**, 1593 (1988).

[6] J. F. Berret, D. C. Roux, and G. Porte, J. Phys. (France) II **4**, 1261 (1994); V. Schmitt, F. Lequeux, A. Poussse, and D. Roux, Langmuir **10**, 955 (1994); R. Cappelaere, R. Cressely, R. Makhloufi, and J. P. Decruppe, Rheol. Acta **33**, 431 (1994).

[7] J. P. Decruppe, R. Cressley, R. Makhloufi, and E. Cappelaere, Colloid Polym. Sci. **273**, 346 (1995); R. Makhloufi, J. P. Decruppe, A. Ait-Ali, and R. Cressley, Europhys. Lett. **32**, 253 (1995).

[8] J. F. Berret, D. C. Roux, G. Porte, and P. Lindner, Europhys. Lett. **25**, 521 (1994).

[9] I. Furo and B. Halle, Phys. Rev. E **51**, 466 (1995).

[10] A. C. Maggs, D. Mukamel, and C. A. Pillet, Phys. Rev. E **50**, 774 (1994).

[11] P. Schurtenberger and C. Cavaco, J. Phys. (France) II **3**, 1279 (1993); **4**, 305 (1994); Langmuir **10**, 100 (1994).

[12] S. Q. Wang, W. M. Gebart, and A. Ben-Shaul, J. Phys. Chem. **94**, 2219 (1990).

[13] S. Q. Wang, J. Phys. Chem. **94**, 8381 (1990).

[14] S. Q. Wang, Macromolecues **24**, 3004 (1991).

[15] H. Rehage, I. Wunderlich, and H. Hoffmann, Prog. Colloid Polym. Sci. **72**, 51 (1986); I. Wunderlich, H. Hoffmann, and H. Rehage, Rheol. Acta **26**, 532 (1987). H. Rehage and H. Hoffmann, J. Phys. Chem. **92**, 4712 (1988).

[16] M. E. Cates and S. T. Milner, Phys. Rev. Lett. **62**, 182 (1989).

[17] N. A. Spenley, M. E. Cates, and T. C. B. McLeish, Phys. Rev. Lett. **71**, 939 (1993).

[18] S. Hoffmann, A. Rauscher, and H. Hoffmann, Ber. Bunsenges. Phys. Chem. **95**, 153 (1991).

[19] B. O'Shaughnessy and J. Yu, Phys. Rev. Lett. **74**, 4329 (1995).

[20] K. Kremer and G. S. Grest, J. Chem. Phys. **92**, 5057 (1990).

[21] M. Kröger, W. Loose, and S. Hess, J. Rheol. **37**, 1057 (1993).

[22] M. Kröger, *Rheologie unde Struktur von Polymerschmelzen* (Wissenschaft and Technik, Berlin, 1995).

[23] S. Hess, J. Non-Newt. Fluid Mech. **23**, 305 (1987).

[24] W. Loose and S. Hess, Rheol. Acta **28**, 91 (1989).

[25] M. Kröger, Rheology **5**, 66 (1995).

[26] W. G. Hoover, Physica A **194**, 450 (1993).

[27] H. M. Laun, R. Bung, S. Hess, W. Loose, O. Hess, K. Hahn, E. Hädicke, R. Hingmann, F. Schmidt, and P. Lindner, J. Rheol. **36**, 743 (1992).

[28] W. Loose and S. Hess, Rheol. Acta **28**, 91 (1989).

[29] J. D. Weeks, D. Chandler, and H. C. Andersen, J. Chem. Phys. **54**, 5237 (1971).

[30] H. R. Warner, Ind. Eng. Chem. Fund. **11**, 379 (1972).

[31] D. Ceperly, M. H. Kalos, and J. L. Lebowitz, Phys. Rev. Lett. **41**, 313 (1978).

[32] J. C. Sexton and D. H. Weingarten, IBM Technical Report No. RC 17668, 1992 (unpublished).

[33] M. P. Allen and D. J. Tildesley, *Computer Simulation of Liquids* (Clarendon, Oxford, 1987).

[34] D. J. Evans, Mol. Phys. **37**, 1745 (1979).

[35] G. S. Grest, B. Dünweg, and K. Kremer, Comput. Phys. Commun. **55**, 269 (1989).

[36] P. J. Missel, N. A. Mazer, G. B. Benedek, C. Y. Young, and M. C. J. Carey, Phys. Chem. **84**, 1044 (1980).

[37] P. J. Mukerjee, Phys. Chem. **76**, 565 (1972).

[38] J. N. Israelachvili, D. J. Mitchell, and B. W. Ninham, J. Chem. Soc. Faraday Trans. II **72**, 1525 (1976).

[39] P. Schurtenberger, C. Cavaco, F. Tiberg, and O. Regev, Langmuir (to be published).

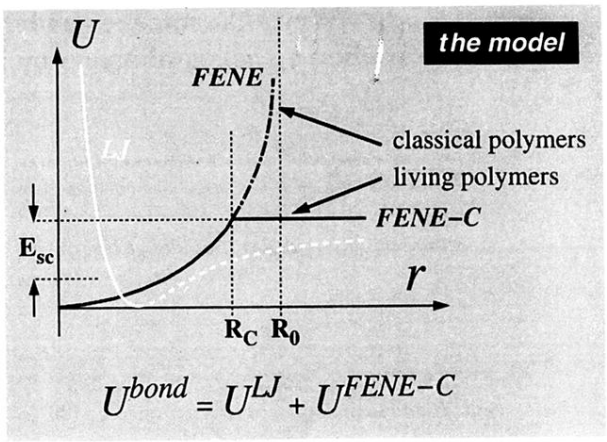

FIG. 1. Model potentials specifying the microscopic model of wormlike micelles. All particles interact via the truncated (repulsive) Lennard-Jones potential. The FENE-C potential produces the bonding interactions.